

# Polycondensation of Boron- and Nitrogen-Codoped Holey Graphene Monoliths from Molecules: Carbocatalysts for Selective Oxidation\*\*

Xin-Hao Li\* and Markus Antonietti

The development of low-cost sustainable catalysts with high stability and excellent catalytic activity under mild conditions remains at the heart of modern materials chemistry and green chemistry.<sup>[1–5]</sup> Carbocatalysts (metal-free and heterogeneous carbon materials) show great potential as sustainable catalysts both for organic synthesis and as electrocatalysts in fuel cells owing to their relatively low cost and their comparable activity to that of commercial platinum catalysts.<sup>[2–4]</sup> Among the carbon allotropes, the high surface area and acceptable stability of modified graphenes make them good candidates for carbon catalysis.<sup>[4]</sup> More importantly, the relative versatility possible in the chemical modification of graphene sheets affords them tunable electronic properties; this simple but efficient approach for tuning their catalytic activity on the atomic level is promising.<sup>[4–6]</sup>

Engineering of the hexagonal crystal lattice of graphene sheets through substitutional doping is thereby a direct way to control the electronic structure/transport properties of graphenes and expands their application in catalysis and electronic devices remarkably.<sup>[4–6]</sup> The insertion of heteroatoms into the graphene lattice to tune the position of the valence band or conduction band of the doped carbon materials results in altered function and a slightly opened band gap; for this purpose, boron was been widely used as an electron acceptor, and nitrogen and phosphorus as electron donors.<sup>[5,6]</sup> Current methods for the mass production of doped graphenes are limited to the chemical modification of layered graphite oxides (GOs). These approaches usually lead to only a low surface area ( $< 300 \text{ m}^2 \text{ g}^{-1}$ ) and a low dopant content of the resulting chemically modified graphenes (CMGs). Despite tremendous efforts, the larger-scale production of homogeneously doped graphene lattices with higher concentrations of these dopants still remains a great challenge for materials scientists. The bottom-up chemical synthesis of doped graphenes from small precursor molecules seems to be the most suitable approach to the tuning of their composition and morphology through the choice of appropriate precursors.<sup>[7]</sup>

In view of the two-dimensional (2D) structure of graphene with its very large aspect ratio, a slight aggregation of graphene layers during and/or after catalytic reactions is inevitable and significantly decreases the number of catalytically active sites exposed to substrates in the following reaction.<sup>[8]</sup> Mass transfer is a standard problem of lamellar materials, as organic molecules cannot transfer through sheets, and even barrier properties are built up. In principle, the generation of nanoholes in the graphene sheets is favorable, as it not only increases the amount of active edges, but also improves mass transfer during catalysis.<sup>[8b,c]</sup> A powerful synthesis therefore includes the possibility of generating through-plane nanopores in doped or pristine graphene sheets.

Herein, we report a one-step chemical approach to the direct synthesis of gram quantities of doped graphene monoliths with nanopores. By this method, we could simultaneously introduce high concentrations of heteroatoms and through-plane nanopores into the graphene structure. Through the copolymerization of glucose and boric acid within the interlayers of lamellar carbon nitrides in a simple thermal pyrolytic process (Figure 1), a boron- and nitrogen-

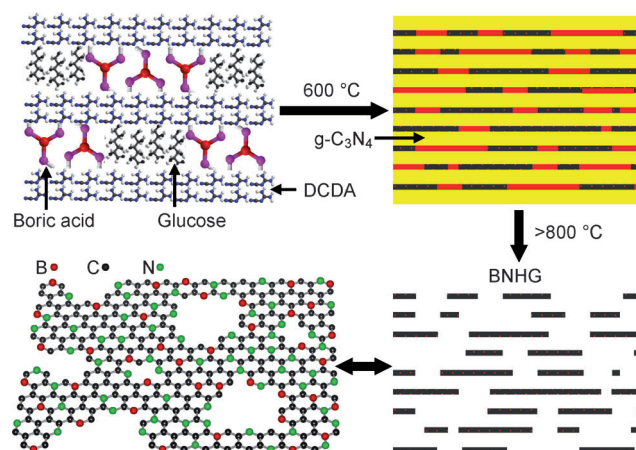


Figure 1. Proposed protocol for the synthesis of BNHG.

codoped holey graphene assembly (BNHG) with a high surface area ( $978 \text{ m}^2 \text{ g}^{-1}$ ) was obtained. A synergistic effect of N and B on the stability, dopant concentration, and catalytic activity of the BNHG was observed. Even after the calcination of the precursor at  $1000^\circ\text{C}$ , the as-formed BNHG still had a very high dopant concentration exceeding 15 atom %. This material shows great potential as a carbocatalyst for organic synthesis. For example, BNHG can efficiently activate oxygen (1 atm) at very low temperatures for the

[\*] Dr. X. H. Li, Prof. M. Antonietti  
Department of Colloid Chemistry  
Max Planck Institute of Colloids and Interfaces  
Research Campus Golm, 14476 Potsdam (Germany)  
E-mail: xin-hao.li@mpikg.mpg.de

[\*\*] This research was supported by the L2H project of the BMBF, the EnerChem project, and the UNICAT project. X.H.L. thanks Prof. X. C. Wang and J. S. Zhang of Fuzhou University for TEM measurements and Dr. Q. S. Gao of the MPIKG for fruitful discussions.

Supporting information for this article is available on the WWW under <http://dx.doi.org/10.1002/anie.201209320>.

oxidative coupling of amines with high selectivity, compatibility, and reusability.

As depicted in Figure 1, BNHG was typically prepared simply by heating a mixture of dicyandiamide (DCDA, 40 g), glucose (1 g), and boric acid (0.4 g) above 800 °C under the protection of flowing N<sub>2</sub> gas. The doping level with B and N atoms was controlled by varying the heating temperature. The samples obtained by heating at 800, 900, and 1000 °C were named BNHG800, BNHG900, and BNHG1000, respectively.

Large-area scanning electron microscopy (SEM) images (see Figure S1a in the Supporting Information) revealed that the as-obtained BNHG materials are assemblies of continuous, flexible, wrinkled sheets. The holey structure of BNHG becomes obvious under higher magnification (see Figure S1b,c). Further transmission electron microscopy (TEM) analysis (Figure 2a; see also Figure S2) and a dark-field TEM image (Figure 3, left) confirmed the uniform 2D structure of the layered carbon with through-plane holes and excluded the presence of condensed particles or a condensed bulk speci-

men. Holes with a size between several nanometers and hundreds of nanometers were observed (Figure S2b,d). The synthesis was not optimized to control the pore size. We proved that boric acid was the dominating factor in inducing the formation of holes by using borazane, borazine, and other boranes as additives; these alternative additives caused no obvious hole formation (data not shown). The acid character of boric acid (which tends to form strong contacts through an electrostatic interaction with ammonia groups of carbon nitride) and its layered structure in the solid phase make boric acid a suitable "template" to generate carbon-poor areas (shown schematically in red in Figure 1) between the as-formed aromatic carbon intermediates (highlighted in black in Figure 1) in the interlayer space of layered carbon nitride. Subsequent thermolysis of the hybrid solid liberated the graphenes and opened the through-plane pores.

HRTEM images (Figure 2b; see also Figure S4) revealed the formation of only very small graphene domains with a size of a few nanometers, which matched well with the very broad G and D peaks found by Raman analysis (see Figure S5). The SAED pattern of the same area (Figure 2c) revealed the typical pattern observed for multicrystalline materials. The broad XRD peaks of BNHG1000 further indicated only restricted stacking in the *c* direction (see Figure S3). The lamellar stacking distance of BNHG1000 was estimated to be 0.32 nm on the basis of the very broad (002) peak centered at 27.2°, which is smaller than that of ideal graphite (0.34 nm). This result speaks for the homogeneous inclusion of B and N atoms in the graphene planes and secondary acid–base interactions between the layers.

X-ray photoemission spectroscopy (XPS) analysis unambiguously excluded the presence of metal components in the BNHG samples (see Figure S6). The introduction of B and N atoms into the graphene framework was also demonstrated by elemental-mapping images (Figure 3) and XPS analysis (see Figure S6) of the as-obtained BNHG monoliths, whereas the UV/Vis absorption spectra of BNHG (see Figure S7) without an obvious absorption edge at 218 nm excluded the formation of pristine boron nitride domains. Homogeneous heteroatom doping of graphene was shown by elemental mapping of any selected area (Figure 3; see also Figure S8). The C 1s XPS spectrum of the BNHG1000 sample (see Figure S9a) indicated significant modifications of the sp<sup>2</sup> carbon atom with heteroatoms through the formation of C–B, C–C, and C–N bonds.<sup>[6]</sup> The N 1s XPS peak (see Figure S9b) demonstrates that the N atoms are inserted into the graphene lattice mainly in the form of "pyridinic" and "graphitic" N atoms and N–B bonds.<sup>[6,7c]</sup> The binding energy of the B 1s orbital (see Figure S9c) of around 190.8 eV indicated the formation of C–B and N–B bonds.<sup>[6]</sup> A minor amount of B–O bonds were also observed; these bonds terminate the layers, as was further confirmed by solid-state NMR spectroscopic analysis (see Figure S10). The total heteroatom content of BNHG1000 is 14 atom% and 16 atom% for B and N, respectively, according to XPS analysis (see Figure S6 and Table S1 in the Supporting Information). The heating temperature had a significant effect on the concentration of B and N atoms; higher temperatures resulted in lower dopant concentrations. Moreover, a certain amount of oxygen was present in the

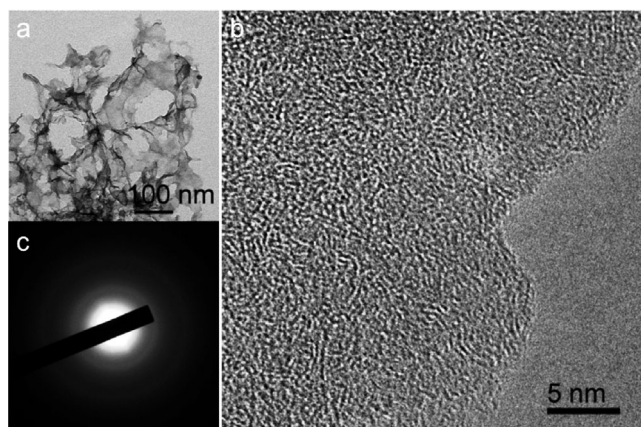


**Figure 2.** a) TEM image of BNHG1000; b) HRTEM image of the edge area; c) selected area electron diffraction (SAED) pattern of the edge area.

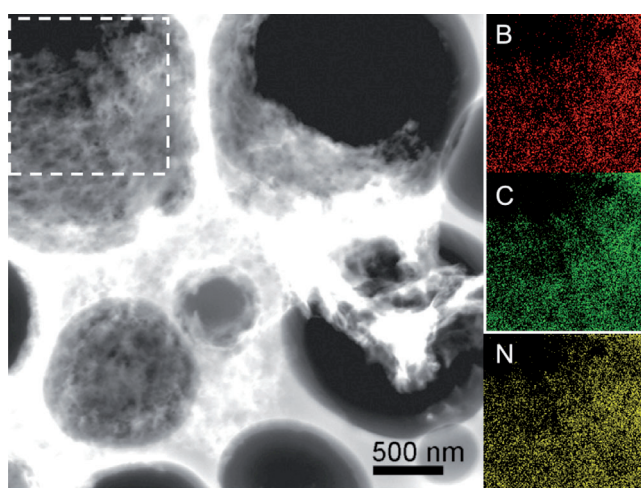


**Figure 3.** Dark-field TEM image of the BNHG1000 monolith (left), and the corresponding boron, carbon, and nitrogen elemental-mapping images of the selected area in the square.

BNHG samples, mainly in the form of O=C–O or H–O–H bonds (see Figure S9d),<sup>[8]</sup> and could not be changed significantly by varying the heating temperature. We attribute the presence of oxygen to strongly chemisorbed oxygen-containing components, presumably CO<sub>2</sub> and H<sub>2</sub>O.<sup>[8]</sup> This phenomenon is general for high-surface-area aromatic carbons, which show super-adsorption toward gases (as seen by a spontaneous mass increase after their release from a vacuum); on the other hand, this property facilitates their application as catalysts to activate gases (especially polarizable gases, such as O<sub>2</sub>, CO<sub>2</sub>, and NO) and organic molecules for catalytic conversion.

The specific surface area of the BNHG samples increased with the heating temperature; in contrast, a higher heating temperature only decreased the specific surface area of pristine or N-doped graphenes, as demonstrated by us in a previous study.<sup>[7c]</sup> The Brunauer–Emmett–Teller (BET) surface area of BNHG1000 was determined to be 978 m<sup>2</sup> g<sup>−1</sup> by nitrogen-adsorption–desorption analysis (see Figure S11). This value corresponds to a calculated average number of layers of 3, as averaged over the complete sample. Simultaneously, the synergetic effect of B and N enhanced not only the chemical stability of the dopant atoms (to remain in the structure) but also the thermal stability of the BNHG monoliths as such. BNHG1000 has a higher surface area as compared with pristine graphenes (821 m<sup>2</sup> g<sup>−1</sup>) obtained under the same conditions without boric acid,<sup>[7c]</sup> and the surface areas of both are higher than that of B- and N-codoped graphenes obtained by the post-treatment of GO (<300 m<sup>2</sup> g<sup>−1</sup>).<sup>[5]</sup> Thus, our copolymerization method has advantages for the bottom-up preparation of doped graphenes.

A number of carbon or carbon nitride nanoallotropes have already shown their great potential as metal-free catalysts for the activation of O<sub>2</sub> or air for selective oxidation, which is of great importance in organic synthesis.<sup>[2–4,9]</sup> As a graphene-based carbocatalyst, GO with its high surface area and its myriad of oxide functionalities has been a benchmark carbocatalyst with fascinating catalytic properties for selective oxidation.<sup>[4]</sup> As GO itself has only moderate stability under conditions of photoirradiation or higher temperature,<sup>[10]</sup> an excess amount of the GO catalyst and highly oxidative reaction conditions (high pressure of O<sub>2</sub> and higher reaction temperatures) have usually been required to avoid the reduction of GO and thus to ensure catalytic activity.

Our BNHG monoliths have high thermal stability (the samples were obtained at temperatures above 800 °C), a high surface area, a high dopant concentration, and good dispersibility in various solvents (see Figure S12) and are simple to make in high yield at a low cost. We therefore tested the catalytic reactivity of BNHG as a sustainable carbocatalyst for catalytic oxidation.

We focused our initial studies on the oxidative coupling of amines to form imines, which are important intermediates in organic synthesis,<sup>[4,9]</sup> under mild conditions: at a low temperature (<100 °C) and a low laboratory pressure of O<sub>2</sub> (1 atm). BNHG, GO, N-doped graphene monoliths (NGr),<sup>[7c]</sup> and reduced GO (RGO) were compared as catalysts. All showed good selectivity for the formation of the imine, but the conversion varied under the standard reaction conditions

(Table 1). GO offered good conversion and slightly lower selectivity for the imine even in the absence of O<sub>2</sub> (Table 1, entries 2 and 3), which indicated that GO underwent a chemical reaction with the substrate under mild conditions.<sup>[4d]</sup> No

**Table 1:** Study of reaction conditions.<sup>[a]</sup>

Entry	Catalyst	Conversion [%] <sup>[b]</sup>	Selectivity [%] <sup>[b]</sup>
1	–	–	–
2	GO	72	95
3	GO (N <sub>2</sub> )	46	97
4	NGr	17	88
5	BNHG800	45	98
6	BNHG900	48	> 99
7	BNHG1000	91	> 99
8	BNHG1000 (N <sub>2</sub> )	–	–
9	RGO	10	91
10 <sup>[c]</sup>	BNHG1000	91	> 99
11 <sup>[d]</sup>	BNHG1000 (2nd cycle)	91	> 99
12 <sup>[d]</sup>	BNHG1000 (3rd cycle)	91	> 99
13 <sup>[d]</sup>	BNHG1000 (4th cycle)	89	> 99

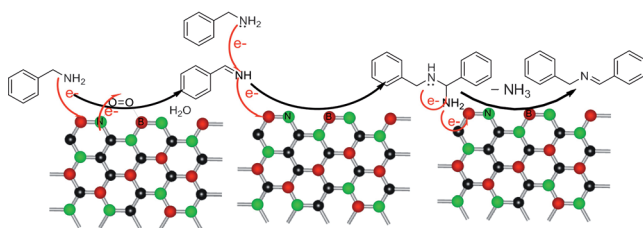
[a] Standard reaction conditions: acetonitrile (5 mL), substrate (1 mmol), catalyst (30 mg), O<sub>2</sub> balloon (1 atm), 4 h, 85 °C. [b] The conversion and selectivity were determined by GC–MS by using aniline as an internal standard. [c] The free-radical scavenger butylated hydroxytoluene (BHT; 10 mol %) was added. [d] The BNHG1000 catalyst (30 mg) was reused for multiple cycles.

conversion was observed without a catalyst (Table 1, entry 1). BNHG could activate O<sub>2</sub> for the transformation of the amine into an imine with very high selectivity (>99 %); its catalytic activity depended on the condensation temperature of the material and thus on its surface area and composition (Table 1, entries 5–7). No reaction was observed in the absence of O<sub>2</sub> (Table 1, entry 8); this result underlines the occurrence of a catalytic reaction over BNHG. Without any cocatalysts, BNHG1000 gave the best conversion (91 %) into the corresponding imine within 4 h under quite mild conditions. Thus, BNHG1000 showed outstanding potential as a sustainable carbocatalyst for O<sub>2</sub> activation or air-based catalytic oxidation. Also, both the conversion and selectivity over BNHG1000 were much higher than those observed with GO under mild conditions.

However, a high surface area and a high dopant concentration are not enough to ensure the catalytic activity of graphene-based catalysts. The fact that NGr, with a similar N-dopant concentration (15.4 atom %) and a very high surface area (916 m<sup>2</sup> g<sup>−1</sup>), could only offer very low conversion and moderate selectivity for the imine product demonstrated the importance of B atoms in enhancing the catalytic activity of the BNHG materials. The introduction of doping atoms into graphite-based materials can induce electron relocalization in both the conduction band (CB) and the valence band (VB) and thus make them appropriate catalysts for oxidation.<sup>[4h]</sup> Similarly, B atoms (as electron acceptors) and N atoms (as electron donors) could in principle lower the VB (or HOMO) and elevate the CB (or LUMO)<sup>[5b,c]</sup> and thus induce electron relocalization to activate the substrate and oxygen molecules



for oxidation reactions. It is believed that the catalytic activity and selectivity are derived from the electronic structure of the HOMO of BNHG1000, as controlled by the N and B heteroatoms, whereas the high surface area and holey structure are beneficial for mass transfer. The failure of a free-radical scavenger (BHT, 10 mol%) to quench the oxidation of benzylamine over BNHG1000 (Table 1, entry 10) revealed that  $O_2$  is activated directly on the surface of the catalyst for the oxidation reactions, without the formation of free radicals (e.g. superoxide radicals) in the solution. Since no overoxidation products of the amine, such as aldehydes and ketones, were detected in the GC–MS spectra of the products, we propose the formation of an amination intermediate, which can readily lose  $NH_3$  to give the imine coupling product (Scheme 1).<sup>[9d]</sup>



**Scheme 1.** Proposed reaction process over BNHG1000.

As the best catalyst for the selective oxidation of benzylamine in this study, BNHG1000 also exhibited excellent reusability and stability. Used BNHG1000 still offered nearly the same catalytic activity in three subsequent cycles of the catalytic reaction under the standard conditions (Table 1, entries 11–13). Although aggregation and the collapse of the 2D layers of used BNHG1000 monoliths were inevitable owing to high-speed stirring (during the reaction) and centrifugation (after the reaction), the holey structure of the primary 2D layers of BNHG1000 provided sufficient diffusion pathways for the dissolved  $O_2$  and organic molecules and thus maintained the catalytic activity of the reused catalyst.

Moreover, our catalysts were generally effective in the aerobic oxidative coupling of amines with different substituents (see Table S2). All reactions proceeded to the corresponding products with relatively high conversion and very high selectivity. Thus, BNHG1000 showed high chemoselectivity and functional-group tolerance in the oxidation of amines.

In conclusion, we have reported the direct copolymerization of glucose and boric acid into B- and N-codoped holey graphene monoliths in high yield (around 60% as calculated on the basis of added carbon from glucose) and at a low cost. This method is simple and versatile for the mass production of high-quality doped graphenes (with a high surface area, a high doping level, and uniform morphology) in a controlled manner and thus paves the way for the large-scale application of these materials. As a green but efficient carbocatalyst, holey BNHG1000 showed excellent catalytic activity and reusability in the activation of  $O_2$  for selective oxidation reactions under mild conditions, as exemplified in this study by the oxidative coupling of amines. These materials have

great potential as catalysts, electrochemical catalysts, or electrode materials for further applications.

## Experimental Section

Typical synthesis of BNHG1000: Dicyandiamide (40 g), monohydrate glucose (1 g), and boric acid (0.4 g) were dissolved in deionized water (200 mL) and stirred at 80 °C to remove water. The resulting white powder was transferred into a crucible, heated at a rate of 2.4 °C min<sup>-1</sup> to 600 °C, and then tempered at this temperature for another 2 h under a flow of nitrogen. The material was then heated further at a rate of 3.3 °C min<sup>-1</sup> to 1000 °C (or 800 °C for BNHG800, or 900 °C for BNHG900) and maintained at that temperature for 1 h. The sample was then allowed to cool naturally to room temperature under the protection of  $N_2$ .

Received: November 21, 2012

Published online: March 25, 2013

**Keywords:** aerobic oxidation · carbocatalysts · dopants · graphene · porous carbon

- [1] For example, see: a) D. A. Nicewicz, D. W. C. MacMillan, *Science* **2008**, 322, 77; b) M. S. Chen, M. C. White, *Science* **2010**, 327, 566; c) L. Kesavan, R. Tiruvalam, M. H. Ab Rahim, M. I. bin Saiman, D. I. Enache, R. L. Jenkins, N. Dimitratos, J. A. Lopez-Sanchez, S. H. Taylor, D. W. Knight, C. J. Kiely, G. J. Hutchings, *Science* **2011**, 331, 195; d) Y. H. Li, S. Das, S. L. Zhou, K. Junge, M. Beller, *J. Am. Chem. Soc.* **2012**, 134, 9727; e) Q. S. Gao, C. Giordano, M. Antonietti, *Angew. Chem.* **2012**, 124, 11910; *Angew. Chem. Int. Ed.* **2012**, 51, 11740.
- [2] For example, see: a) J. Zhang, X. Liu, R. Blume, A. H. Zhang, R. Schlögl, D. S. Su, *Science* **2008**, 322, 73; b) D. S. Su, J. Zhang, B. Frank, A. Thomas, X. C. Wang, J. Paraknowitsch, R. Schlögl, *ChemSusChem* **2010**, 3, 169, and references therein; c) K. K. R. Datta, B. V. Basireddy, K. Ariga, A. Vinu, *Angew. Chem.* **2010**, 122, 6097; *Angew. Chem. Int. Ed.* **2010**, 49, 5961; d) R. Liu, S. M. Mahurin, C. Li, R. R. Unocic, J. C. Idrobo, H. J. Gao, S. J. Pennycook, S. Dai, *Angew. Chem.* **2011**, 123, 6931; *Angew. Chem. Int. Ed.* **2011**, 50, 6799; e) Y. Wang, X. C. Wang, M. Antonietti, *Angew. Chem.* **2012**, 124, 70; *Angew. Chem. Int. Ed.* **2012**, 51, 68, and references therein; f) X. H. Li, X. C. Wang, M. Antonietti, *ACS Catal.* **2012**, 2, 2082; g) X. Liu, B. Frank, W. Zhang, T. P. Cotter, R. Schlögl, D. S. Su, *Angew. Chem.* **2011**, 123, 3376; *Angew. Chem. Int. Ed.* **2011**, 50, 3318; h) F. Goettmann, A. Fischer, M. Antonietti, A. Thomas, *Angew. Chem.* **2006**, 118, 4579; *Angew. Chem. Int. Ed.* **2006**, 45, 4467.
- [3] a) W. Yang, T.-P. Fellingner, M. Antonietti, *J. Am. Chem. Soc.* **2011**, 133, 206; b) T.-P. Fellingner, F. Hasché, P. Strasser, M. Antonietti, *J. Am. Chem. Soc.* **2012**, 134, 4072; c) Y. Li, W. Zhou, H. Wang, L. Xie, Y. Liang, F. Wei, J.-C. Idrobo, S. J. Pennycook, H. Dai, *Nat. Nanotechnol.* **2012**, 7, 394; d) D.-S. Yang, D. Bhattacharjya, S. Inamdar, J. Park, J.-S. Yu, *J. Am. Chem. Soc.* **2012**, 134, 16127.
- [4] a) D. R. Dreyer, H.-P. Jia, C. W. Bielawski, *Angew. Chem.* **2010**, 122, 6965; *Angew. Chem. Int. Ed.* **2010**, 49, 6813; b) D. R. Dreyer, C. W. Bielawski, *Chem. Sci.* **2011**, 2, 1233, and references therein; c) X. H. Li, J. S. Chen, X. C. Wang, J. H. Sun, M. Antonietti, *J. Am. Chem. Soc.* **2011**, 133, 8074; d) H.-P. Jia, D. R. Dreyer, C. W. Bielawski, *Tetrahedron* **2011**, 67, 4431; e) H. Huang, J. Huang, Y. M. Liu, H. Y. He, Y. Cao, K.-N. Fan, *Green Chem.* **2012**, 14, 930; f) J. L. Long, X. Q. Xie, J. Xu, Q. Gu, L. M. Chen, X. X. Wang, *ACS Catal.* **2012**, 2, 622; g) H.-P. Jia, D. R. Dreyer, C. W. Bielawski, *Adv. Synth. Catal.* **2011**, 353, 528;

- h) D. R. Dreyer, H.-P. Jia, A. D. Todd, J. X. Geng, C. W. Bielawski, *Org. Biomol. Chem.* **2011**, 9, 7292.
- [5] a) X. R. Wang, X. L. Li, L. Zhang, Y. Yoon, P. K. Weber, H. L. Wang, J. Guo, H. J. Dai, *Science* **2009**, 324, 768; b) S. Y. Wang, E. Iyyamperumal, A. Roy, Y. H. Xue, D. S. Yu, L. M. Dai, *Angew. Chem.* **2011**, 123, 11960; *Angew. Chem. Int. Ed.* **2011**, 50, 11756; c) S. Y. Wang, L. P. Zhang, Z. H. Xia, A. Roy, D. W. Chang, J.-B. Baek, L. M. Dai, *Angew. Chem.* **2012**, 124, 4285; *Angew. Chem. Int. Ed.* **2012**, 51, 4209; d) Z.-S. Wu, A. Winter, L. Chen, A. Turchanin, X. L. Feng, K. Müllen, *Adv. Mater.* **2012**, 24, 5130.
- [6] a) L. J. Ci, L. Song, C. H. Jin, D. Jariwala, D. X. Wu, Y. J. Li, A. Srivastava, Z. F. Wang, K. Storr, L. Balicas, F. Liu, P. M. Ajayan, *Nat. Mater.* **2010**, 9, 430; b) W. W. Lei, D. Portehault, R. Dimova, M. Antonietti, *J. Am. Chem. Soc.* **2011**, 133, 7121.
- [7] a) J. M. Cai, P. Ruffieux, R. Jaafar, M. Bieri, T. Braun, S. Blankenburg, M. Muoth, A. P. Seitsonen, M. Saleh, X. L. Feng, K. Müllen, R. Fasel, *Nature* **2010**, 466, 470; b) L. Dössel, L. Gherghel, X. L. Feng, K. Müllen, *Angew. Chem.* **2011**, 123, 2588; *Angew. Chem. Int. Ed.* **2011**, 50, 2540; c) X. H. Li, S. Kurasch, U. Kaiser, M. Antonietti, *Angew. Chem.* **2012**, 124, 9827; *Angew. Chem. Int. Ed.* **2012**, 51, 9689; d) A. Götzhäuser, *Angew. Chem.* **2012**, 124, 11095; *Angew. Chem. Int. Ed.* **2012**, 51, 10936, and references therein.
- [8] a) Y. W. Zhu, S. Murali, M. D. Stoller, K. J. Ganesh, W. W. Cai, P. J. Ferreira, A. Pirkle, R. M. Wallace, K. A. Cychosz, M. Thommes, D. Su, E. A. Stach, R. S. Ruoff, *Science* **2011**, 332, 1537; b) X. Zhao, C. M. Hayner, M. C. Kung, H. H. Kung, *ACS Nano* **2011**, 5, 8739; c) Z. P. Chen, W. C. Ren, L. B. Gao, B. L. Liu, S. F. Pei, H.-M. Cheng, *Nat. Mater.* **2011**, 10, 424.
- [9] a) H. C. Brown, Y. Okamoto, *J. Am. Chem. Soc.* **1958**, 80, 4979; b) A. Grirrane, A. Corma, H. García, *Science* **2008**, 322, 1661; c) F. Z. Su, S. C. Mathew, L. Möhlmann, M. Antonietti, X. C. Wang, S. Blechert, *Angew. Chem.* **2011**, 123, 683; *Angew. Chem. Int. Ed.* **2011**, 50, 657; d) B. L. Zhu, M. Lazar, B. G. Trewyn, R. J. Angelici, *J. Catal.* **2008**, 260, 1.
- [10] X. H. Li, J. S. Chen, X. C. Wang, M. E. Schuster, R. Schlögl, M. Antonietti, *ChemSusChem* **2012**, 5, 642.